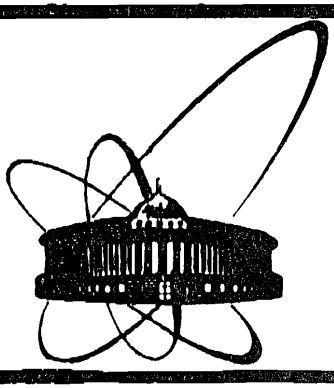

объединенный
институт
ядерных
исследований
дубна

E2-86-471

B.Z.Kopeliovich

MECHANISMS OF $\bar{p}p$ INTERACTION AT LOW AND HIGH ENERGIES

Submitted to "ЯФ"

1986

1. Introduction

The growth of hadronic total cross sections at high energies is most simply described in the Regge phenomenology by introducing the Pomeron pole with intercept above unity[1]. Leading logarithm calculations[2,3] in QCD showed indeed that the vacuum singularity (more complicated than a simple pole[3,4]) is displayed above unity.

The partial amplitude in the impact parameter ($\vec{b}$) representation has the form

$$f(b) = f(0)\exp(-b^2/2B) \qquad (1)$$

and grows with energy because

$$f(0) = i\alpha\nu^{\Delta}. \qquad (2)$$

Here $\nu = 2m_N E/s_0$, is the incident energy in the lab. system; $s_0 = 1\ GeV^2$; $\Delta = \alpha_{I\!P}(0)-1$.

The simplest way to restore the unitary violated by (1) and (2) is to sum up the eikonal graphs with multipomeron exchange[1]. The eikonalized amplitude takes the form

$$F(b) = i\left\{1 - \exp[if(b)]\right\}. \qquad (3)$$

The substitution of (1) into (3) leads to a rapid growth with energy of the slope parameter $B_{eff} \equiv \frac{1}{2}\langle b^2\rangle$:

$$B_{eff} = \frac{1}{2} B\Delta \ln\nu. \qquad (4)$$

Amplitude (3) corresponds to the scattering on a "black disk" of radius $R^2 = 2B\Delta\ln\nu$.

It is interesting that an analogous pattern takes place in low energy $\bar{p}p$ interaction. Indeed, the elastic scattering amplitude is almost imaginary. As the energy decreases, a growing contribution of reggeons (ω,f) and annihilation channels to the amplitude $f(b)$ violates the unitary.

As a result, the impact parameter dependence of amplitude (3) differs considerably from the gaussian form. Indeed, in the latter case the partial amplitude at a zero impact parameter can be written as

$$ImF(0) = 4\sigma_{el}/\sigma_{tot}. \qquad (5)$$

The results of substitution of the experimental data[5] into the right-hand side of this relation are shown in fig.1. It is seen that in the momentum range $P_L \lesssim$ 10 GeV/c the gaussian form of the partial amplitude $F(b)$ contradicts the unitary.

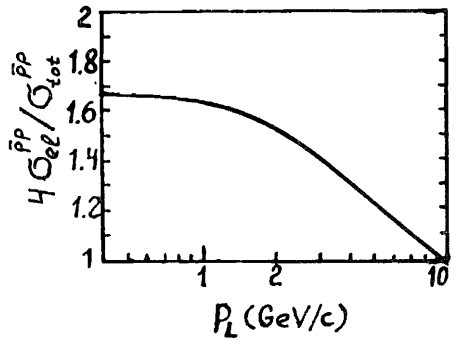

Fig.1.

The ratio $4\sigma_{el}^{\bar{p}p}/\sigma_{tot}^{\bar{p}p}$ as a function of the momentum.

In fact, as is shown below, the $\bar{p}p$ elastic scattering at low energies corresponds to the "black disk" limit. In Sec.2 the experimental data on $\bar{p}p$ total cross section are fitted with the unitarized expression (3) for the scattering amplitude.

In Sec. 3 and 4 the total and differential elastic cross sections and slope parameter are calculated without any free parameter. The results are in good agreement with experimental data. It is worth noting that $\sigma_{el}^{\bar{p}p}$ and B_{eff} at low energies are close to the "black disc"-limit values $\sigma_{el}^{\bar{p}p} = \sigma_{tot}^{\bar{p}p}/2$ and to $B = \sigma_{tot}^{\bar{p}p}/4\pi$, respectively.

As phases of different contributions to the elastic amplitude are connected with their energy dependence, it is possible to estimate the ratio of the real part of the forward elastic scattering amplitude to the imaginary part. The calculations performed in Sec. 5 are in good agreement with experimental data.

The problem of the high-energy-annihilation mechanism is considered in Sec.6. It is shown that the mechanism of the string junction annihilation within a perturbation theory corresponds to the double gluon exchange in the decuplet state. But the comparison of the corresponding Regge trajectory intercepts reveals serious disagreement. The experimental data analysis performed in the momentum range $P_L \lesssim 12$ GeV/c (which may not be asymptotic) gives results

corresponding to none of the above-mentioned theoretical treatments.

2. Total cross section

From (3) one can easily obtain the following expression for the total cross section

$$\sigma_{tot} = 4\pi B\{C + \ln[\mathrm{Im} f(0)] - E_i[-\mathrm{Im} f(0)]\}. \quad (6)$$

Here $C=0.5772$ is the Euler constant; $E_i(-z)$ is an integral exponential function.

The amplitude of $\bar{P}P$ scattering at high energies $p_L \gtrsim 10$ GeV/c is dominated by the Pomeron contribution (Fig.2a)

$$\mathrm{Im} f_{I\!P}(0) = a\,\nu^{\Delta} \quad (7)$$

and the Reggeon one (Fig. 2b)

$$\mathrm{Im} f_R(0) = b/\sqrt{\nu}. \quad (8)$$

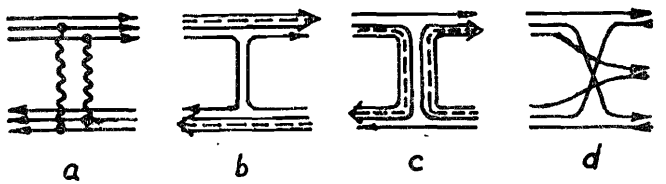

Fig.2.

The graphs included in the fit of the total cross section.

In the fitting procedure the slope parameters of all contributions were taken to be equal to

$$B = B_0 + 2\alpha'_{I\!P}\ln\nu. \quad (9)$$

Parameter B_0 is determined by the nucleon form factor and is connected with the nucleon mean square radius: $B_0 = 2\langle r_N^2\rangle/3 \approx 10.8\ \mathrm{GeV}^{-2}$. At the same time the fit[4] of the data for the slope parameter in the pp ($\bar{p}p$) elastic scattering gives $B_0 = 8.9 \div 10.2\ \mathrm{GeV}^{-2}$. We fixed the value of

$B_0 = 10\ \mathrm{GeV}^{-2}$. The parameters Δ and $\alpha'_{I\!P}$ have also been fixed[4]. The corresponding values and the results of fitting the parameters a and b are given in the Table.

Table

Values of the parameters of the input amplitude $f(b)$. Fixed parameters are marked by the star

Δ	$\alpha_R(0)$	$\alpha'_{I\!P}$	B_0	a	b	c	d	e	h	g
0.1*	0.5*	0.13*	10*	0.39	3.71	23.73	0.0046	2.58	1.95	0.75
			GeV^{-2}	GeV^{-2}	±0.001	±0.03	±0.05	±0.0002	±0.02	±0.03	±0.05

At lower energies the annihilation contribution becomes considerable. The energy dependence of the planar annihilation graph shown in Fig. 2c is determined by the intercept $\alpha_{D\bar{D}}(0)$ of the trajectory corresponding to exotic diquark-antidiquark meson states. $\alpha_{D\bar{D}}(0)$ can be found by using known nucleon and meson trajectory intercepts. The corresponding contribution to the input amplitude $f(b)$ has the form

$$\mathrm{Im} f_{D\bar{D}}(0) = c\,\nu^{2\alpha_N(0)-\alpha_R(0)-1}. \quad (10)$$

This contribution is well determined in the momentum range $1 \lesssim p_L \lesssim 10$(GeV/c). It is worth noting that extension of the Regge asymptotics to the low-energy region is admissible because the c.m. energy of the intermediate $q\bar{q}$ state is still quite high at the threshold.

In the near-threshold momentum range the recombination mechanism of annihilation (Fig.2d) becomes to be important[7]. We parametrized this contribution in the form

$$\mathrm{Im} f_{rec}(0) = d/k^e, \quad (11)$$

where $k = \sqrt{m_N E/2 - m_N^2}$ is the $\bar{p}p$ c.m. momentum. The results of fitting the parameters c, d, e are reported in the Table.

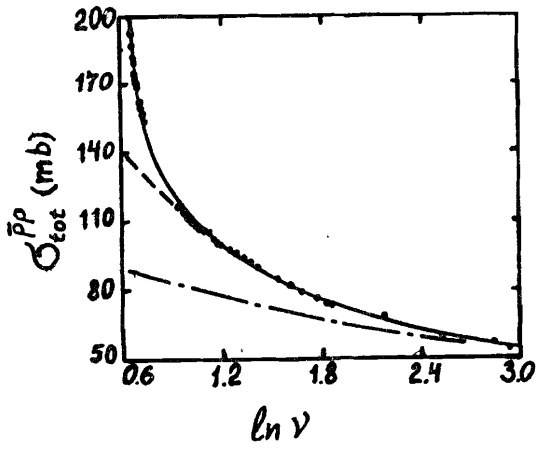

Fig.3.

The $\bar{p}p$ total cross section. The solid curve is the fit result; The line-dotted (dashed) curve is the same but without contribution of graphs in Fig. 2c,e (Fig. 2d). The experimental points are from ref./5,8/

The calculated curves are compared with experimental data/5,8/ in Fig.3. It is important that the energy dependence of the diquark-exchange contribution defining the corss section in the range $1 \lesssim p_L \lesssim$ 10 (GeV/c) is proved to be correct.

3. Elastic scattering cross section

It is known from the experimental data (see Sec.5) that the real part of the scattering amplitude is small. Thus, the elastic cross section $\sigma_{el}^{\bar{p}p}$ can be expressed as

$$\sigma_{el}^{\bar{p}p} = \int d^2b\,|F(b)|^2 = 2\pi B\left\{C + \ln[\mathrm{Im}\,f(0)/2] + \right.$$
$$\left. + E_i[-2\,\mathrm{Im}\,f(0)] - 2\,E_i[-\mathrm{Im}\,f(0)]\right\}. \qquad (12)$$

The result of calculation of $\sigma_{el}^{\bar{p}p}$ with the parameter values fixed in the Table is shown in Fig.4. A good agreement of calculation with the experimental data/5/ is an important evidence for the "black disk" regime. In the "gray disk" case $\sigma_{el}^{\bar{p}p}$ would be smaller.

The possibility calculating $\sigma_{el}^{\bar{p}p}$ knowing the value of $\sigma_{tot}^{\bar{p}p}$ only is nontrivial. For instance, in the case of a gaussian form of the amplitude $F(b)$ one should also know the value of slope parameter B_{eff} which is very large at low energies (see the next Sec).

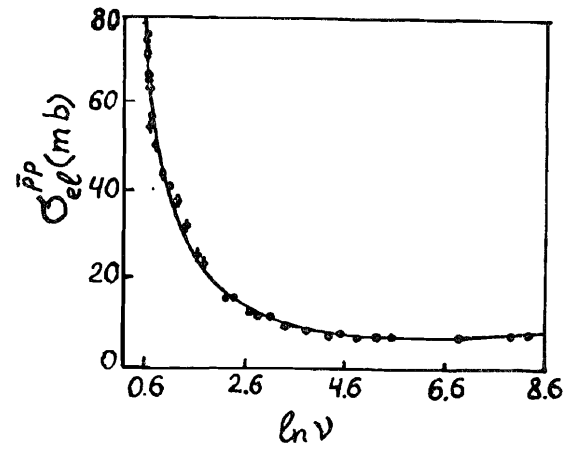

Fig.4.

Elastic $\bar{p}p$ scattering cross section. Data points are from compilation/5/. The curve shows the result of calculation with parameters fixed in the Table.

Here we have only used the known value of the nucleon radius.

4. Elastic scattering differential cross section

The effective slope defined as $B_{eff} = d\ln(d\sigma_{el}/dq^2)/dq^2\big|_{q=0}$ in the case of amplitude (3) has the form

$$B_{eff} = \frac{1}{2}\langle b^2\rangle = \frac{8\pi B^2}{\sigma_{tot}^{\bar{p}p}}\int_0^{\mathrm{Im}\,f(0)}\frac{dx}{x}\left[C + \ln x - E_i(-x)\right]. \qquad (13)$$

The momentum dependence of B_{eff} calculated with parameters from the Table is compared with the experimental data/9-12/ in Fig.5. One can see now that large value of B_{eff} at low energies is a result of the unitarization, i.e. self-screening of the processes with a large cross section.

The value of the effective slope contains only some averaged information about the process. A more serious test is the comparison of calculations with the data on the angular dependence of the differential cross section.

For the partial amplitude (3) the differential cross section can be written as

$$\frac{d\sigma}{d\Omega_{c.m.}} = B^2k^2\left|\int_0^{\mathrm{Im}\,f(0)}\frac{dx}{x}\left(1-e^{-x}\right)J_0(qb)\right|^2. \qquad (14)$$

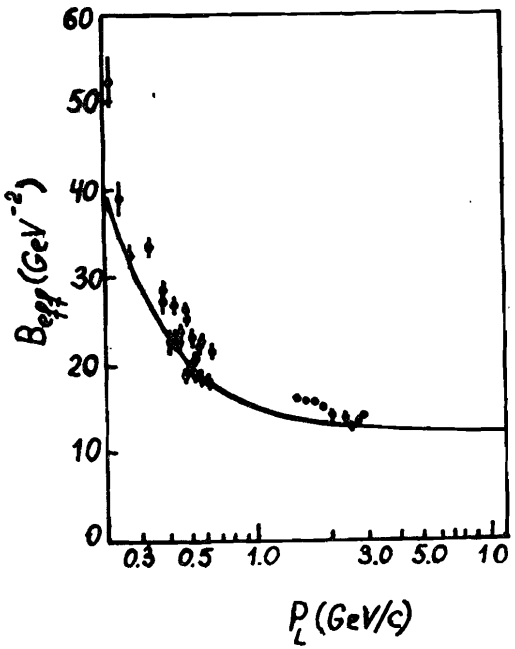

Fig.5.

Effective slope of the elastic $\bar{p}p$ scattering. The curve is the calculation result with parameters from Table. Data points are taken from ref./9-12/.

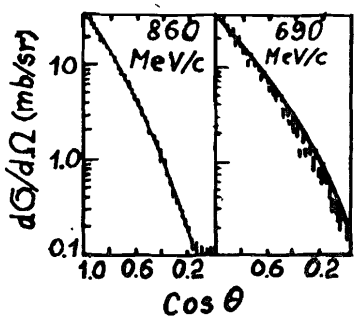

Fig.6.

Elastic scattering differential cross section. The experimental points are taken from ref./13/. The curve is calculated with parameters from the Table.

(14)

Here k is the $\bar{p}p$ c.m. momentum; $J_0(z)$ is the Bessel function; $q^2 = 2k^2(1-\cos\theta)$; $b = 2B\ell n[\mathrm{Im}f(0)/x]$.

The comparison of the calculation with experimental data/13/ in Fig.6 displays a good agreement up to a large angles $\sim 90^\circ$.

5. Real part of the forward scattering amplitude

Let us consider the contribution of the graphs shown in Fig.2 to the real part of the forward $\bar{p}p$ elastic scattering amplitude. Graphs 2a and 2b give almost imaginary contribution because the first one has an interesept close to one, and the second one is cancelled in the real part of the amplitude due to the exchange degeneracy of reggeons. But the diquark exchange contribution (Fig.2c) has a nonzero

real part. Indeed, the ratio $\rho_{D\bar{D}} = \mathrm{Re}\, f_{D\bar{D}}(q)/\mathrm{Im}\, f_{D\bar{D}}(q)\big|_{q=0}$ (in the case of exchange degeneracy) is equal to

$$\rho_{D\bar{D}} = \frac{1}{2}\left[\mathrm{tg}\frac{\pi\alpha_{D\bar{D}}(0)}{2} - \mathrm{ctg}\frac{\pi\alpha_{D\bar{D}}(0)}{2}\right]. \qquad (15)$$

As was mentioned above (see (10)), $\alpha_{D\bar{D}}(0) = 2\alpha_N(0) - \alpha_R(0) = -1.3$ if $\alpha_N(0) = -0.4$. The corresponding value of $\rho_{D\bar{D}}$ from (15) is $\rho_{D\bar{D}} = 0.73$. Note a high sensitivity of $\rho_{D\bar{D}}$ to the $\alpha_N(0)$ value. If, for instance, one sets $\alpha_N(0) = -0.35$, he finds $\rho_{D\bar{D}} = 1.38$.

The diquark-exchange contribution to the amplitude is given by the following expression

$$\rho = \frac{4\pi B}{\sigma_{tot}^{\bar{p}p}} \int_0^{\mathrm{Im}f(0)} \frac{dx}{x} e^{-x} \sin\left[x\rho_{D\bar{D}}\mathrm{Im}\, f_{D\bar{D}}(0)/\mathrm{Im}\, f(0)\right]. \qquad (16)$$

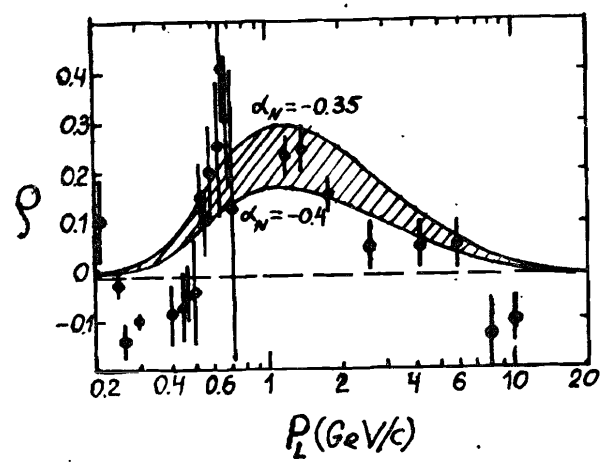

Fig.7.

The ratio of imaginary part of the forward elastic scattering amplitude to the real one. Experimental points are taken from refs. /9-11,14/. Solid curves are results of the calculation with parameters from the Table and $\alpha_N(0) = -0.35$, $\alpha_N(0) = -0.4$.

The calculation contains no free parameters except those fixed in the Table. The results are compared with data/9-11,14/ in Fig. 7. Two curves corresponding to $\alpha_N(0) = -0.35$ and $\alpha_N(0) = -0.4$ demonstate the sensitivity of ρ to the $\alpha_N(0)$ value.

Note that the momentum dependence of ρ is typical for the "black disk" limit. Indeed, while the momentum is decreased in a few GeV/c range, the Fig. 2c diagram contribution grows and the value of ρ becomes large. But as the momentum decreases below 1 GeV/c, other

annihilation contributions become dominant and shadow the real part of diagram in fig.2c. Thus, the value of ρ tends to zero. At smaller momenta the real part of the amplitude is determined by an unknown contribution of the recombination mechanism.

The agreement of our predictions for the real part of the amplitude with the experimental data is an essential argument in favour of correctness of the diquark exchange energy dependence and existence of the "black disk" regime. Note that the results obtained are not a consequence of the analyticity but only of the chosen form of F(b). Dispersion relations do not give any reliable prediction in this energy range (see, for instance[15]).

6. Annihilation at high energies

The $\bar{p}p$ annihilation at high energies is described in dual models[6,16] as a result of the string junction exchange. The simplest diagrams are shown in Figs. 2c and 8. The dotted line denotes the string junction. The diagram in Fig. 8b dominates in asymptotics. It corresponds to the three-jet configuration which has the mean particle multiplicity 3/2 times as large as that of the cilinder diagram.

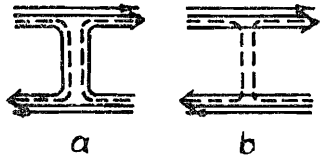

Fig.8.

Dual annihilation diagrams.

The energy dependence of the Fig.8b diagram contribution to the total cross section is described by ν^{λ}, where[6]

$$\lambda = 2\alpha_N(0) - 3\alpha_R(0) + 1 \approx -1.3. \qquad (17)$$

In the annihilation channel at high energies one should introduce a suppression factor $K(\nu) = \exp(-3\langle n_{N\bar{N}}\rangle)$, where $\langle n_{N\bar{N}}\rangle$ is an average multiplicity of $N\bar{N}$ pairs in one jet. It is clear that this factor forbids the $N\bar{N}$ production from see. It is known from experiment that $\langle n_{N\bar{N}}\rangle \approx 0.1\langle n_{\pi}\rangle$, where $\langle n_{\pi}\rangle$ is pion average multiplicity which is approximately equal to $2[1-\alpha_R(0)]\ln\nu$. Factor 2 takes into account that pions mostly originate from vector meson decays.

Thus, the contribution of graph 8b to the annihilation channel differs from the contribution to the total cross section by a factor

$$K(\nu) \approx \nu^{-0.3}. \qquad (18)$$

Let us now examine these problems from a perturbative point of view. The exchange during interaction by two gluons which are in a colour decuplet state leads to formation of two quark systems in the final state: decuplet, $3q$ and antidecuplet, $3\bar{q}$. It is clear that such systems inevitably desintegrate into the jets, i.e. contribute to the annihilation. The Regge intercept corresponding to the decuplet exchange has been calculated in paper[18]

$$\alpha_{10}(0) = 1 - \frac{3g^2}{8\pi^2}, \qquad (19)$$

where g is the QCD coupling constant. The pomeron intercept in the same approximation is $\alpha_{I\!P}(0) = 1 + 3g^2\ln 2/\pi^2$. This value can be estimated from analysis[4] of the experimental data: $\Delta_{I\!P} = \alpha_{I\!P}(0) - 1 \approx 0.3$*). Consequently, $\Delta_{10} = -\Delta_{I\!P}/8\ln 2 \approx -0.05$, i.e. the decuplet trajectory intercept does not practically differ from unity.

The difference between (19) and (17) is significant. It is difficult to suggest that it can be reduced by reggeization of the double decuplet exchange contribution to the elastic amplitude. One can assume, of course, that the decuplet exchange in perturbation theory and the string junction annihilation in the dual model are different phenomena. But this conclusion is very strange. It is worth recalling that value (17) is strongly model-dependent, and expression (19) is obtained in the region where parturbation theory is invalid. Thus, the question is still open.

Let us try to extract the effective intercept value directly from the experimental data[5] on annihilation cross section. Only two diagrams 2c and 2d from those included into fit of the total cross section contribute to the annihilation. But this one falls off too rapidly with the energy growth. Let us introduce supplementary

*) The pomeron approximation by two poles with $\alpha(0)=1$ and $\alpha(0) = 1+\Delta$ has been considered in ref./4/. Such a variant is more appropriate for the QCD calculation[19] than a single-pole approximation used here in sect.2 for simplicity.

term into the annihilation amplitude which should describe the high energy behaviour:

$$\mathrm{Im}\, f_{an} = b/\sqrt{s} + c\, \nu^{2\alpha_N(0)-\alpha_R(0)-1} + h/\nu^{q}. \qquad (20)$$

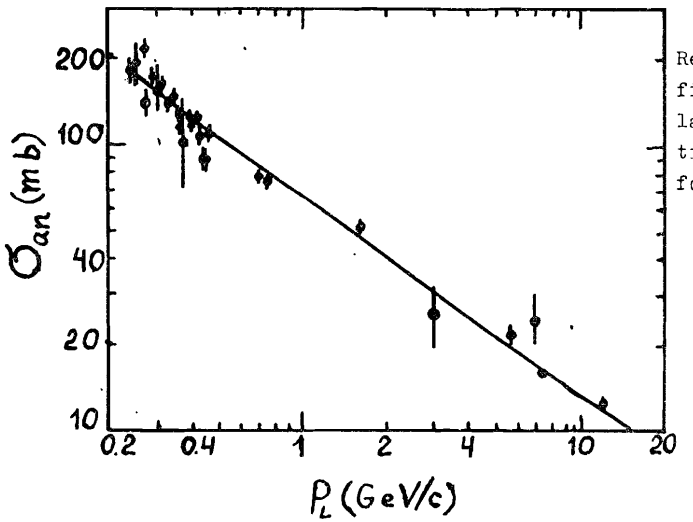

Fig. 9. Results of the fit to the annihilation cross section data[5] by the formula (21).

The parameters b and c have been fixed in the Table. The values of h and q are determined from fitting the experimental-data[5] by the following expression

$$\sigma_{an} = 2\int d^2b\, \exp[-\mathrm{Im} f(b)]\left\{\exp[\mathrm{Im} f_{an}(b)] - 1\right\} - \int d^2b\, \exp[-2\,\mathrm{Im} f(b)]\left\{\exp[\mathrm{Im} f_{an}(b)] - 1\right\}. \qquad (21)$$

The results of the fit (h=1.95 and q=0.75) are shown in Fig.9. Note that inclusion of a new term into the annihilaton amplitude (20) does not essentially influence the total cross section because the energy behaviour of this term is close to that of the amplitude $f_R(\nu)$, i.e. it has been effectively contained in the elastic amplitude $f(b)$.

The momentum range of the existing data[5] is restricted by value 12 GeV/c which is below the $N\bar{N}$ production threshold for 3-jet events. Thus, factor (18) should not be introduced.

Value q =0.75 found from the fit considerably differs both from (7) and the value $2\alpha_{10}(0) - 2$ given by (19). The effective intercept value is equal to $\alpha_{eff}(0) = 1 - q$ =0.25.

It is obvious that the momentum 12 GeV/c may be far from the asymptotical region and the value of $\alpha_{eff}(0)$ may have nothing to do with the diagram in Fig.8b. Thus, the data on the annihilation cross section at higher energies are extremely necessary. There exists also a problem of the annihilation contribution to the $p\bar{p}$ and pp total-cross-section difference[16]. In connection with this question it is desirable to study the process[16] of pp-interaction with nucleon pair production in the fragmentation region of one of the incident protons. This channel can be described as a result of the string junction[16] (or decuplet) exchange in the pp scattering. It is interesting that the energy behaviour (17) of this reaction cross section in the dual scheme is close to the nucleon exchange one. Just the nucleon exchange is responsible in the Regge phenomenology for the transition of the baryon quantum number through a large rapidity gap.

7. Conclusion

The analysis performed here shows that dynamical origine of the large value of the $\bar{p}p$ slope parameter is the unitarization of the elastic scattering amplitude. The impact parameter pictures of $\bar{p}p$ scattering at low and superhigh energies are very similar. Fitting the total cross section we predicted low energy values of the slope parameter, elastic cross section and real part of the forward elastic scattering amplitude in good agreement with experimental data. This set of results testifies to the existence of the "black disk" limit in $\bar{p}p$ interaction at low energies. The analysis confirmed also the correctness of the diquark exchange energy dependence.

Note that the unitarization scheme is not unique. Once can consider, for example, the amplitude in the form

$$F(b) = \frac{f(b)}{1 - i f(b)}. \qquad (22)$$

The agreement of the elastic cross section and real part of the amplitude with experimental data in this case is not so good as for the eikonal unitarization (3).

It is worth noting the importance of correct usage of the amplitude $F(b)$ in Glauber-like calculations of the $\bar{p}$-nuclei interaction cross section at low energies. It is known,[4] that the usage of a gaussian amplitude $F(b)$ at superhigh cosmic-ray energies produces a considerable error in the hadron nuclei cross sections.

The latter comment concerns the possibility of existence of the baryonium[19]. Due to the "blackness" the annihilation amplitude fully shadows all other channels of $\bar{p}p$ scattering in the interaction range $b^2 \lesssim 2B_{eff}$. At momenta $p_L \lesssim 0.3$ GeV/c the shadow has a transverse dimension larger than 2 fm.

This work was essentially stimulated by helpful discussions with L.I.Lapidus and his interest in the subject. I am grateful also to M.G.Sapozhnikov who informed me about interesting properties of interaction at low energies and supplied with some experimental data.

References:

1. Dubovikov M.S., Kopeliovich B.Z., Lapidus L.I., Ter-Martirosyan K.A., Nucl.Phys. 1976, B123, p147.
2. Balitsky Ya.Ya., Lipatov L.N., Fadin V.S., "Elementary Particle Physics", LNPI, Leningrad, 1979, p.109.
3. Lipatov L.N., Preprint LNPI-1137, Leningrad, 1985.
4. Kopeliovich B.Z., Nikolaev N.N., JINR-E2-86-125, Dubna, 1986.
5. Flaminio V. et al., Compilation of cross-sections III: p and $\bar{p}$ induced reactions, CERN-HERA, 84-01, Geneva, 1984.
6. Ross G.C., Veneziano G., Nucl.Phys., 1977, B123 p507.
7. Maruyama M., Tamotsu V., Prog. of Theor. Phys., 1985, 73, p1211. Green A.M., Preprint HU-TFT-85-11, Helsinki, 1985.
8. Beard C.I. et.al., Preprint CERN-EP/84-140, 1984.
9. Bruckner V. et.al., Phys.Lett., 1985, 158B, p.180.
10. Cresti M., Peruzzo L., Sartori G., Phys.Lett., 1983, 123B, p.209.
11. Ashford V. et.al., Phys.Rev.Lett., 1985, 54, p518.
12. Parker D. et al., Nucl. Phys., 1971, B32, p29.
13. Eisenhandler et al., Nucl.Phys., 1976, B113, p1.
14. Iwasaki H. et.al., Nuc. Phys., 1985, A433, p.580.
15. Kondratiuk L.A., Sapozhnikov M.G., "Atomic Nuclear Physics", LNPI, Leningrad, 1985, p.297.
16. Volkovitsky P.E., Preprint ITEP-128, Moscow, 1985.
17. Kopeliovich B.Z., Lapidus L.I., Proc. of Int. Conf. on High Energy Nuclear Physics., Balatonfured, Hungary, 1983, p73.
18. Bronzan J.B., Sugar R.L., Phys. Rev., 1978, D17, p2813.
19. Shapiro I.S., Phys.Repts., 1978, 35c, p129.

Received by Publishing Department
on July 7, 1986.

Б.З.Копелиович Е2-86-471

Механизмы взаимодействия антипротонов при низких и высоких энергиях

Показано, что большой радиус взаимодействия $\bar{p}p$ при низких энергиях есть следствие унитаризации амплитуды рассеяния - явление, аналогичное тому, что ожидается при сверхвысоких энергиях. В обоих случаях амплитуда рассеяния имеет форму "черного диска". Без свободных параметров вычислены наклон и дифференциальное сечение упругого рассеяния, реальная часть амплитуды рассеяния вперед. Обсуждается вопрос о механизме аннигиляции при высоких энергиях.

Работа выполнена в Лаборатории теоретической физики ОИЯИ.

Препринт Объединенного института ядерных исследований. Дубна 1986

Kopeliovich B.Z. E2-86-471

Mechanisms of $\bar{p}p$ Interaction at Low and High Energies

It is shown that large radius of $\bar{p}p$ interaction at low energies is the result of the scattering amplitude unitarization, analogous to that believed at superhigh energies. In both cases partial amplitude takes a form of "black" disk in the impact parameter space. After fitting the total cross section, the slope, the total and differential elastic cross section, the real part of the forward elastic scattering amplitude are calculated without any new parameters. The mechanisms of $\bar{p}p$ annihilation at high energies are also considered.

The investigation has been performed at the Laboratory of Theoretical Physics, JINR.

Preprint of the Joint Institute for Nuclear Research. Dubna 1986